IMPROVEMENT OF CYGNSS LEVEL 1 CALIBRATION USING MODELING AND MEASUREMENTS OF OCEAN SURFACE MEAN SQUARE SLOPE

Tianlin Wang[1], Valery U. Zavorotny[2], Joel Johnson[3], Yuchan Yi[3], Christopher Ruf[1], Scott Gleason[4], Darren McKague[1], Paul Hwang[5], Erick Rogers[6], Shuyi Chen[7], Yulin Pan[1], Thomas Bakker[1]

[1]University of Michigan, Ann Arbor, MI USA
[2] Cooperative Inst. for Research in Environmental Sciences, University of Colorado, Boulder, CO USA
[3]The Ohio State University, Columbus, OH USA
[4]University Corporation for Atmospheric Research, Boulder, CO USA
[5]Naval Research Laboratory, Washington DC, USA
[6]Naval Research Laboratory, Stennis Space Center, MS USA
[7]University of Washington, Seattle, WA, USA

ABSTRACT

The Cyclone Global Navigation Satellite System (CYGNSS) measures GPS signals specularly reflected from Earth's surface to remotely sense ocean surface roughness and wind speed. The mean square slope (mss) is a key physical parameter that relates the ocean surface properties (wave spectra) with the CYGNSS measurement of the normalized bistatic radar cross section (NBRCS). An approach to model the mss for validation with CYGNSS mss data was developed by adding the contribution of a high frequency tail to the IFREMER WAVEWATCH III (WW3) mss. It is demonstrated that the ratio of CYGNSS mss and the modified WW3 mss can be used to diagnose potential calibration errors that exist in the Level 1 calibration algorithm. This approach can help to improve CYGNSS data quality, including the Level 1 NBRCS and Level 2 ocean surface wind speed and roughness.

Index Terms— Calibration, CYGNSS, mean square slope (mss), validation, WaveWatch III, wind speed

1. INTRODUCTION

The Cyclone Global Navigation Satellite System (CYGNSS) performs bistatic scatterometer measurements to obtain information about ocean surface roughness and winds by measuring Delay Doppler maps (DDMs) [1]. The Level 1 calibration algorithm converts the DDMs into the normalized bistatic radar cross section (NBRCS) of the sea surface [2]. The Level 2 retrieval algorithm uses the calibrated NBRCS to retrieve the wind speed and to compute the mean square slope (mss) of the sea surface.

The CYGNSS Level 1 calibration requires knowledge of many parameters, including the transmit power and antenna gain pattern of the GPS transmitters, the receive antenna and receiver system gains, etc. Thus, it is of great importance to detect, isolate and correct any errors existing in the estimate of those parameters to further improve the Level 1 calibration and to provide more accurate Level 2 retrievals.

The characterization of GPS transmitters is being studied using a GPS constellation power monitor (GCPM) system [3, 4] and the direct signal measured by the zenith channel of CYGNSS satellites [5, 6]. The absolute calibration will provide a relatively accurate estimate of the effective isotropic radiated power (EIRP) of the GPS transmitter for CYGNSS's v3.0 algorithm (for data after August 1, 2018).

A correction to the receiver antenna gain pattern was previously derived using anomalies in the NBRCS observations; this correction was applied as part of the V2.1 Level 1 calibration algorithm [7]. However, it is noted that this NBRCS anomaly is considered to be dependent only on the wind speed and specular incidence angle, which may not be true in all cases. It has been demonstrated that the error in wind speeds retrieved from GNSS-Reflectometry (GNSS-R) observations is strongly correlated with the significant wave height (SWH) of the ocean [8]. Hence, there is a necessity to take into account the sea state influence, especially the non-local swell contribution to the ocean surface roughness [9, 10].

A physics-based approach is therefore proposed in this paper to examine potential calibration errors and to further improve the Level 1 calibration. Rather than using the NBRCS anomaly, this approach is based on comparison of the sea surface mss estimated by CYGNSS and a reference mss produced by wave models or in-situ measurements. The baseline algorithm of calculating the reference mss is adding the contribution of a high frequency tail to the IFREMER WAVEWATCH III® (WW3) mss. This method enables us to determine potential anomalies observed in CYGNSS's mss that can then be compared with calibration errors existing in the NBRCS. These studies should help to further improve the calibration quality and the accuracy of Level 2 data products, including both mss and wind speed U_{10}.

2. MEAN SQUARE SLOPE MODELING

The baseline equation used for the CYGNSS Level 2 mss mss_{CY} computation is

$$mss_{CY} = \frac{|R|^2}{\sigma_{CY}} \quad (1)$$

where R is the complex Fresnel coefficient for right-hand circular incidence/left-hand circular scattering, and σ_{CY} is the CYGNSS NBRCS.

The idea is to obtain an mss product either from models or in-situ measurements to compare with the CYGNSS mss as a method for detecting potential calibration errors.

One resource is the IFREMER WW3 model predicted mss. However, this WW3 implementation has a fixed cutoff frequency at κ_{WW3} = 2.1 rad/m in resolving the sea surface spectrum [11], while the CYGNSS-observed mss should be sensitive to contributions from sea waves up to the cutoff frequency

$$\kappa_{CY} = \frac{2\pi \cos\theta_{inc}}{3\lambda} \quad (2)$$

where θ_{inc} is the specular incidence angle and λ is the wavelength for the GPS L1 signal. The typical value of κ_{CY} is from 4 to 12 rad/m.

For a typical case, swell portions of the wave spectrum are narrower in wavenumber, have an amplitude that exceeds that of wind generated waves in the same spectral region, and have a peak wavenumber that resides in the low-frequency (long-wave) region. The wind-sea portion of the spectrum in contrast is wider in wavenumber space, but has a smaller amplitude whose peak position is in the high-frequency (short-wave) region [11-13].

To compare the WW3 and CYGNSS estimated mss, we need to add the portion of wave spectrum (high-frequency 'tail') generated by the local wind from κ_{WW3} to κ_{CY}. Currently, the Elfouhaily *et al.* spectrum [14] is used to model this spectrum. Three parameters are inputs to the model: the "ground-truth" wind speed (from the ECMWF winds that force the WW3 prediction), the specular incidence angle (determining the cutoff frequency), and the inverse wave age Ω_0 for the wind-sea. The latter is estimated using

$$\Omega_0 = \frac{U_c}{c_{p0}} = \frac{2\pi U_{10} cos\theta_{ww}}{gT_{p0}} \quad (3)$$

where θ_{ww} is the angle between wave and wind directions, and T_{p0} is the wave period at the spectral peak for the wind-sea partition.

Empirical models of ocean wave spectra predict that the inverse wave age Ω_0 of local wind seas at finite fetch can be larger than the asymptotic value of 0.84 for infinite fetch [14]. The calculation of Ω_0 using wind speeds and wave periods T_{p0} from IFREMER WW3 data on average support this; however, a portion of realizations yield values of Ω_0 smaller than 0.84, which could be caused by uncontrolled swell contribution into the partition 0 (windsea) spectrum and other complicated factors of wind-sea interaction [9]. For those cases, since we are not able to use the Elfouhaily et al. spectrum to generate the local wind spectra, we remove such cases from the datasets used to assess the calibration process.

The modified WW3 mss is calculated by taking into account the directivity of waves [15] as

$$mss_{mWW3} = 2[mss_{WW3,x}mss_{WW3,y} + mss_{E,x}mss_{E,y} + (mss_{E,x}mss_{WW3,y} + mss_{WW3,x}mss_{E,y})cos^2\Delta\theta + (mss_{WW3,x}mss_{E,x} + mss_{WW3,y}mss_{E,y})sin^2\Delta\theta]^{1/2} \quad (4)$$

where the subscript 'WW3' means WaveWatch III, 'E' means the modeled "tail" mss using the Elfouhaily et al. spectrum, and $\Delta\theta$ is the difference between directions of both the wind and the mss distribution.

3. MSS RATIO FOR CALIBRATION DIAGNOSTICS

The mss ratio (*mssR*) is calculated as follows:

$$mssR = \frac{mss_{CY}}{mss_{mWW3}} \quad (5)$$

The dataset used is a subset of the CYGNSS v 3.0 data from days 001 to 334 for the Year 2019. The mss ratio is calculated for individual GPS PRN and CYGNSS Flight Model (FM) numbers to examine the dependence on these parameters. The ratio is also mapped to the receiver antenna coordinate system and binned 1 by 1 degree, and the average within each bin over the dataset is examined.

3.1 mss Ratio for Individual PRN and FM

Fig. 1 shows the mss ratio of CYGNSS FM1 with GPS transmitter PRN11. The histogram shows that there could be potential calibration error on the receive antenna pattern, as patterns are observed in these plots that differ for the starboard and port sides. The mean *mssR* is calculated using a weighted average by the measurement density. Mean mssR for starboard and port antennas are computed separately.

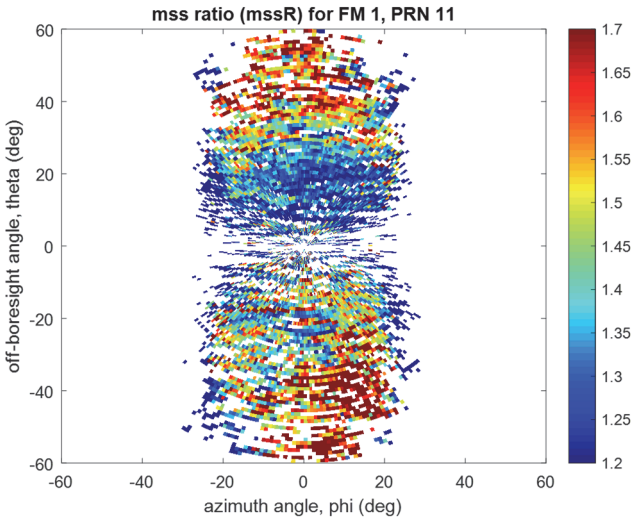

Fig. 1 mss ratio for FM1/PRN11

3.2 mean mssR for Individual PRN and FM

Fig. 2 shows the mean mssR of starboard and port versus GPS for all CYGNSS flight model (FM), with differing colors labeling distinct FM in this case. We can use them to diagnose possible calibration issues existing in the GPS EIRP and the gain of receiver antenna and receiver system. The differences between the starboard and port channels can be identified through inter-comparison of two mean mssR sets.

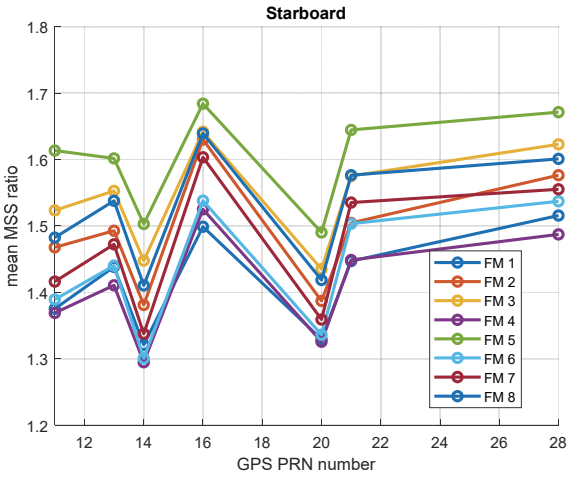

(a)

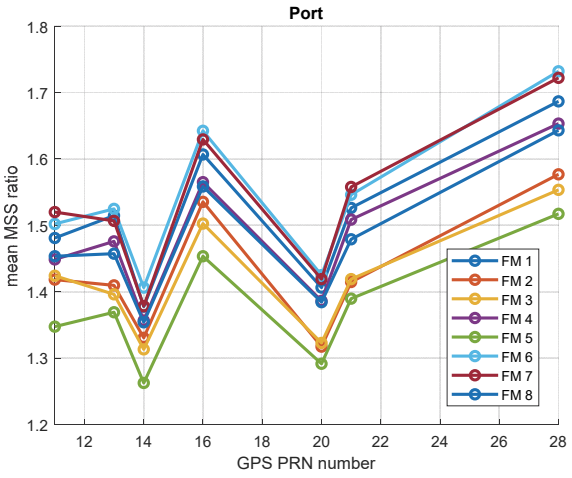

(b)

Fig. 2 Mean *mssR* for mean *mssR* vs. GPS PRN for all CYGNSS FMs. (a) starboard; (b) port.

3.3 Normalized mss Ratio for FM Using Multiple PRNs

The next step is to remove the bias of the individual *mssR* map (normalized by its mean *mssR*) and then merge the normalized maps of multiple PRNs/FM pairs by a weighted average with the measurement density. This allows us to calculate a correction map to the receiver antenna gain pattern. The normalized *mssR* for FM1 using seven Block IIR PRNs are computed from two independent data subsets of the entire dataset. As shown in Fig. 3, the repeatability of the two normalized *mssR* maps demonstrates that it is an engineering calibration issue that needs to be resolved for the receiver antenna pattern.

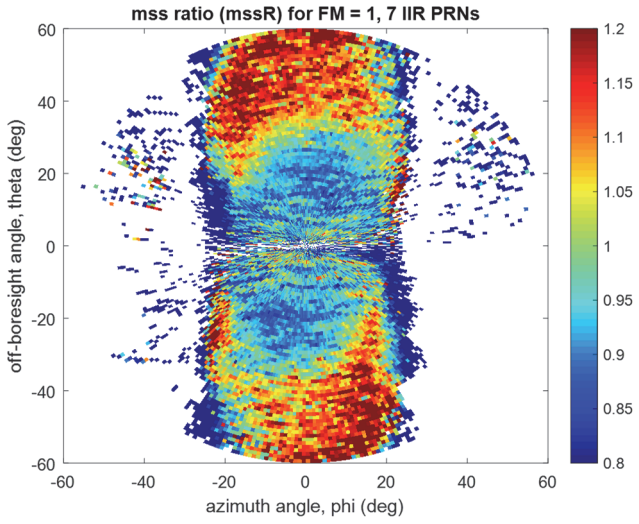

(a)

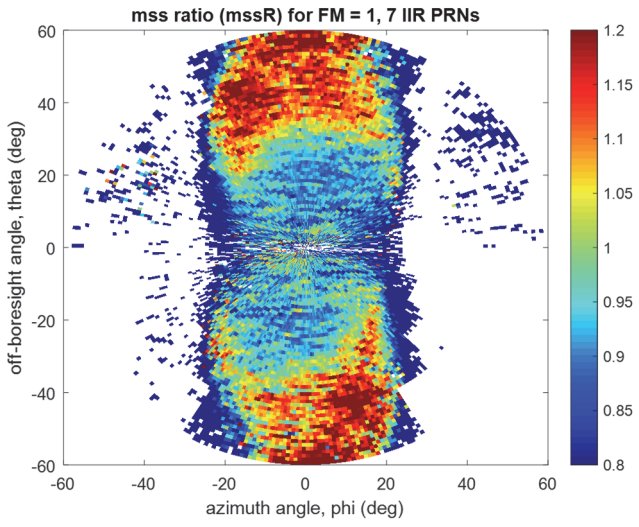

(b)

Fig. 3 Normalized *mssR* for FM1 using 7 Block IIR PRNs. (a) Calculated from data subset 1; (b) calculated from data subset 2. Notice that the color scaled is symmetric about unity, unlike Fig. 2.

4. DISCUSSION ON MODELING THE WAVE TAIL

In this development, the Elfouhaily et al. spectrum is used to model the high frequency tail of the spectrum. However, that method lacks validation with in-situ measurements and also has a limitation with respect to the wind speed and inverse wave age.

The CYGNSS wave-model working group is currently investigating possibilities of developing a more accurate model for the high-frequency tail of the spectrum and validating the modeling using buoy measurements. The alternate approach under consideration include the spectrum integration method [16], the Unified Wave INterface-Coupled Model (UWIN-CM) [17], and in-situ buoy observations, etc. This aims to provide more accurate matchup mss for improving CYGNSS Level 1 calibration and also for validation of CYGNSS's Level 2 mss product.

5. SUMMARY

An approach for using modified WaveWatch III predicted mss to improve CYGNSS Level 1 calibration is proposed. The reference mss is produced by adding a high frequency tail (modeled using the Elfouhaily et al. spectrum) to the WW3 mss. By comparing the ratio of CYGNSS measured mss and modified WW3 mss, it has been shown that the mean ratio has a dependence on both GPS PRNs and CYGNSS FMs, as well as each FM's starboard and port channels. The normalized mss ratio map from multiple PRNs calculated from two independent data subsets are strongly repeatable. Therefore it should be an engineering correction factor to be applied on the receiver antenna gain pattern. These indicate potential calibration errors existing in the characterization of the GPS transmitters and the CYGNSS receivers. By correcting these errors, this approach will help to improve the data quality of the CYGNSS Level 1 calibration and the Level 2 wind speed and mss products.

6. REFERENCES

[1] C. S. Ruf, A. Lyons, M. Unwin, J. Dickinson, R. Rose, D. Rose, and M. Vincent, "CYGNSS: Enabling the future of hurricane prediction," *IEEE Geosci. Remote Sens. Mag.*, vol. 1, no. 2, pp. 52-67, June 2013.

[2] Ruf, C. S., et al., *CYGNSS Handbook*, Michigan Publishing, Ann Arbor, MI, 2016.

[3] T. Wang, C. Ruf, S. Gleason, B. Block, D. McKague, and D. Provost, "Development of GPS constellation power monitor system for high accuracy calibration/validation of the CYGNSS L1B data," *2017 IEEE International Geoscience and Remote Sensing Symposium*, Fort Worth, TX, 2017, pp. 1008-1011.

[4] T. Wang, C. S. Ruf, B. Block, D. S. McKague and S. Gleason, "Design and performance of a GPS constellation power monitor system for improved CYGNSS L1B calibration," *IEEE Journal of Selected Topics in Applied Earth Observations and Remote Sensing*, vol. 12, no. 1, pp. 26-36, Jan. 2019.

[5] T. Wang, C. Ruf, B. Block and D. McKague, "Characterization of the transmit power and antenna pattern of the GPS constellation for the CYGNSS Mission," *2018 IEEE International Geoscience and Remote Sensing Symposium*, Valencia, 2018, pp. 4011-4014.

[6] T. Wang, C. Ruf, S. Gleason, D. McKague and A. O'Brien, "A real-time EIRP Level 1 calibration algorithm for the CYGNSS mission using the zenith measurements," *2019 IEEE International Geoscience and Remote Sensing Symposium*, Yokohama, Japan, 2019, pp. 8725-8728.

[7] S. Gleason, C. S. Ruf, A. J. O'Brien and D. S. McKague, "The CYGNSS Level 1 calibration algorithm and error analysis based on on-orbit measurements," *IEEE Journal of Selected Topics in Applied Earth Observations and Remote Sensing*, vol. 12, no. 1, pp. 37-49, Jan. 2019

[8] M. P. Clarizia, C. S. Ruf, "Bayesian wind speed estimation conditioned on significant wave height for GNSS-R ocean observations," *J. Atmos. Ocean. Tech.*, vol. 34, no.6, pp.1193-1202, June 2017.

[9] T. Wang, V. U. Zavorotny, J. Johnson, C. Ruf and Y. Yi, "Modeling of sea state conditions for improvement of CYGNSS L2 wind speed retrievals," *2018 IEEE International Geoscience and Remote Sensing Symposium*, Valencia, Spain, 2018, pp. 8288-8291.

[10] T. Wang, V. U. Zavorotny, J. Johnson, Y. Yi and C. Ruf, "Integration of CYGNSS wind and wave observations with the WaveWatch III numerical model," *2019 IEEE International Geoscience and Remote Sensing Symposium*, Yokohama, Japan, 2019, pp. 8350-8353.

[11] WaveWatch III Development Group, "User manual and system documentation of WaveWatch III version 5.16," *MMAB Technical Note*, Oct. 2016.

[12] Camps, A. et al., "Wind and salinity experiment 2000 (WISE 2000): Scientific analysis report," ESTEC Contract, Aug. 2001.

[13] J. Miranda, M. Vall-Ilossera, A. Camps, and N. Duffo, "Sea surface emissivity at L-band: Swell effects," *IEEE International Geoscience and Remote Sensing Symposium*, Toronto, Ontario, Canada, 2002, pp. 2623-2625.

[14] T. Elfouhaily, B. Chapron, and K. Katsaros, "A unified directional spectrum for long and short wind-driven waves," *J. Geophys. Res.*, vol. 102, no. C7, pp. 15781-15796, July 1997.

[15] V. Zavorotny, "Mean square slope correction for the WW3 MSS entries", unpublished private communication, March 2019.

[16] P. A. Hwang, F. J. Ocampo-Torres and H. García-Nava, "Wind sea and swell separation of 1D wave spectrum by a spectrum integration method," *Journal of Atmospheric and Oceanic Technology*, vol. 29, no. 1, pp. 116-128, 2012.

[17] S. Chen, W. Zhao, M. A. Donelan, and H. L. Tolman, "Directional wind–wave coupling in fully coupled atmosphere–wave–ocean models: Results from CBLAST-Hurricane," *Journal of the Atmospheric Sciences*, vol. 70, no. 10, pp. 3198-3215, 2013.